Special Issue http://dx.doi.org/10.3786/sincs2011.13

NANO-MICRO LETTERS ARTICLE

www.nmletters.org

(Proceedings of 2011 Shanghai International Nanotechnology Cooperation Symposium, SINCS 2011, Published online 10 January 2012)

Investigation of Temperature Annealing Effects on the Optical Properties of ZnO Films by Using Surface Plasmon Resonance

Ming Bao, Hui Wang, Dongmei Jiang, Wenjuan Cheng, Xueming Ma*

Abstract: Surface plasmon resonance (SPR) technique was used to optically characterize ZnO thin films. ZnO films with the thickness of 200 nm have been deposited onto Ag/glass substrates by radio frequency magnetron (RF) sputtering. The as-deposited films were annealed in air at different temperatures from 100℃ to 400℃ for 1 h. By using fitting of the SPR curves with Fresnel's theory, dielectric constant at optical frequency of the prepared thin films were determined. The work shows an efficient method to calculate optical properties of thin film and highlight a promising application of the SPR based system as a temperature sensor.

Keywords: ZnO; Sensing films; Surface plasmon resonance

Citation: Ming Bao, Hui Wang, Dongmei Jiang, Wenjuan Cheng and Xueming Ma, "Investigation of Temperature Annealing Effects on the Optical Properties of ZnO Films by Using Surface Plasmon Resonance", Proceedings of Shanghai International Nanotechnology Cooperation Symposium, 51-56 (2011). http://dx.doi.org/10.3786/sincs2011.13

Introduction

Surface plasmon resonance (SPR) is a quantum optical-electric phenomenon arising from the interaction of light with the oscillation of free electrons that propagates along with the surface bound to a dielectric medium i.e., surface plasmon (SP) [1,2]. SPR technique shows high performance for the sensitive detection of optical properties of thin films and interfaces [3], as well as for biological and chemical sensing [4,5]. The highly surface sensitive nature of the SPR sensor is derived from the unique characteristic of the SPR-generated evanescent field at the metal/dielectric interface under the total internal reflection condition. The evanescent field is strongest at the metal/dielectric interface due to the resonance coupling between the incident radiation and the surface plasmon wave. The evanescent field decays exponentially into both the metal film and the dielectric media. The rapid decay of the evanescent field makes SPR sensor very sensitive to thickness and/or refractive index changes of the adjacent dielectric media next to the metal film [6]. It is believed that a change in the refractive index of the adjacent dielectric media of 10^{-5} may be monitored by SPR [4].

Zinc oxide, ZnO, is a material with great potential for various applications, such as surface acoustic wave devices, optical waveguides, transparent conductive oxides, UV-light emitters, chemical and gas sensors, etc [7,8]. ZnO has been considered as one of most promising candidates for photonic applications in the UV or blue spectra range due to its wide bandgap (≈3.37 eV at room temperature [7] and high exciton-binding energy (60 meV) [7]. It has also been suggested that ZnO exhibits sensing response to C_2H_5OH, C_2H_2, CO, NH_3, O_3 gases, which makes it suitable for sensing applications. Also, good electron transfer, excellent optical properties, and biocompatibility make it suitable for biomedical applications [9,10]. Hense, the optical properties of ZnO film is necessary to realise the photonic devices in the optical frequency range. Many factors

---

State Key Laboratory of Precision Spectroscopy, and Department of Physics, East China Normal University, Shanghai 200062, China
*Corresponding author. E-mail: xmma@phy.ecnu.edu.cn

can affect the properties of ZnO films. Among them, annealing temperature have significant effect on the optical properties of the films and may effect the device performance. Many reports exist in the literature on the influence of annealing temperature on the optical properties of ZnO films. However, the study of the influence of annealing treatment on the optical properties of ZnO films in the optical frequency range has few reports [11,12].

Many deposition techniques have been applied for the fabrication of ZnO films. Sputtering is the most commonly used technique due to its relative high deposition rate, good film properties, low substrate temperature and process stability [13,14].

In this research, the experimental results of dielectric constant, refractive index and packing density of ZnO films after post-annealing treatment process have been investigated by means of the SPR technique, with aim to show the applicability of SPR based system for realization of temperature sensor.

Experimental

ZnO/Ag chips were deposited layer by layer on glass substrate (BK7) using direct current magetron sputtering and radio frequency magnetron sputtering. The base chamber pressure before deposition was pumped to approximately 5×10^{-4} Pa, and the sputtering was carried out at a chamber pressure of about 1 Pa in argon or argon/oxygen atmosphere. Thin silver films (~50 nm) were firstly grown on glass substrates at a constant current of 300 mA at room temperature in an Ar gas atmosphere (10 sccm) to avoid oxidation. ZnO thin films (~200 nm) were deposited on silver coated glass substrates face using rf-sputtering of ZnO target (99.99% pure) at 70 W in a mixture of 2 sccm oxygen, 20 sccm argon at room temperature. After the deposition, the samples were annealed in air at temperature ranging from 100℃ to 400℃ for 1 h. The thickness of the films was measured with a surface profiler. The surface topography of ZnO film deposited onto Ag/glass substrates intended for SPR measurements was inspected by atomic force microscopy, and images were recorded from different areas of the sample surface, at different scan sizes, in order to check the lateral uniformity of the ZnO film.

All measurements of SPR curves were carried out using a SPR equipment consisting of a home-made experimental set-up using Kretschmann's prism configuration [13]. The free face of the glass substrate coated with the ZnO film was brought into optical contact with a prism (with refractive index $n = 1.515$) using a thin layer of an index-matching fluid ($n = 1.517$). The prism/sample combination was placed on a $\theta - 2\theta$ rotation table driven by a microprocessor-controlled stepping motor (with a resolution of 0.01°). Surface plasmon excitation was achieved by directing a p-polarized He-Ne laser ($\lambda = 632.8$ nm) onto the prism/sample interface and measuring the intensity variation of the reflected light as a function of the incident angle.

Results and discussion

Figure 1 reports the atomic force microscopy transversal view image of the as-deposited ZnO layer deposited onto Ag/glass. Scans over different regions of the samples and with different scan lengths indicate an RMS roughness value of 10.5±0.1 nm.

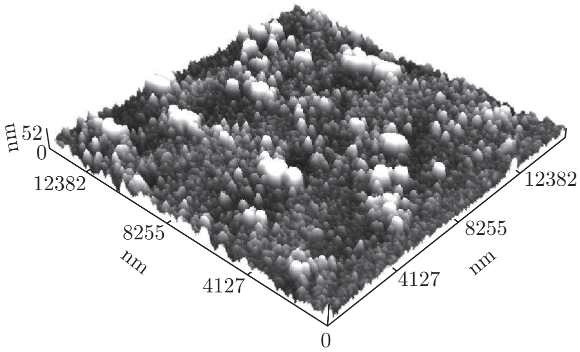

Fig. 1 16 μm×16 μm AFM transversal view image of the as-deposited ZnO layer deposited onto Ag/glass substrate for SPR measurement.

SPR has been shown to be a technique with high sensitivity in charactering ultrathin films at nanometer thickness scale [14]. SPR is a surface characterization technique that takes advantage due to the enhanced evanescent field at the surface of a thin noble metal film for probing thin dielectric film deposited on its surface. In a prism-coupled system, after the optical wave is totally reflected at the prism-metal layer interface, it can be evanescently penetrated through the metal layer and excite the surface plasmon waves (SPW). In this sense, the SPW can retain electromagnetic energy of the incident light due to a resonant energy from incident light to the SPW possible, the wavevectors of both waves should have the same values. Therefore, the prism coupler is used to enhance the momentum of the incident optical wave. The coupling condition may be represented as shown in the following expression:

$$k_x = \sqrt{\varepsilon_0}\frac{2\pi}{\lambda}\sin\theta = \frac{2\pi}{\lambda}\sqrt{\frac{\varepsilon_1'\varepsilon_3}{\varepsilon_1'+\varepsilon_3}}, \tag{1}$$

Where k_x is the wavevector of the incident light, θ represents the incident angle, ε_1' represents the real part of the dielectric constant for the silver film, and ε_3 is the dielectric constant of the solvent (closely of the sensor chip surface).

As a result of this coupling between the incident wave and SPW, the reflectivity plungses dramatically beyond the critical angle. This drop in the reflectivity is well documented resonant energy transfer, and the angle of the minimum is denoted as the surface plasmon resonance angle (θ_{spr}) [15]. Near the resonance angle, an extremely strong evanescent field (EF) is generated at the metal/dielectric interface by the SPW. On the other hand, the properties of EF are governed by the experimental parameters such as dielectric constant of prisms, metal film and dielectric medium, and the thickness of the metal film. Thus, changes of the dielectric constants and/or thickness of the dielectric medium at the vicinity of the metal surface shift the resonance position of the SPR angle [16]. For this reason, SPR technique represents a valid tool for probing the optical constants and thickness of a thin layer deposited onto the thin film metal surface. Typically, the values of the optical parameters are obtained as result of successive numerical fitting of the experimental curve by using the Fresnel equation [14].

In order to properly estimate the optical parameters of the investigated materials by using SPR technique, it is necessary to know them for each layer of the multiple structure. The optical parameters were therefore sequentially determined, starting from the values of the bare silver film, then those of deposited ZnO thin films both as deposited and thermally treated.

In order to know how the SPR curves vary as a function of the optical parameters n and k and thickness d from a theoretical point of view. In this sense, a four-phase system was used in order to simulate the behavior of the reflectivity curves during the excitation of the surface plasmon. In Fig. 2, SPR curves were simulated to verify the effects of thickness and complex refractive index of the silver film on the properties of the SPR spectra, for a p-polarized incident wave with wavelength $\lambda = 632.8$ nm. For calculation purposes, refractive indices of 1.0 and 1.515 for the ambient medium and the prism respectively were assumed. The comparison of these curves shows how the behaviour of surface layer SPR curve can be related to the variation of the optical parameters. As can be observed, increase in n results a reduction of the depth of the resonant curve, similarly to what observed for decrease in d. Moreover, decrease in d not only alters the position of the resonance angle but also broadens the SPR curve to higher incident angles.

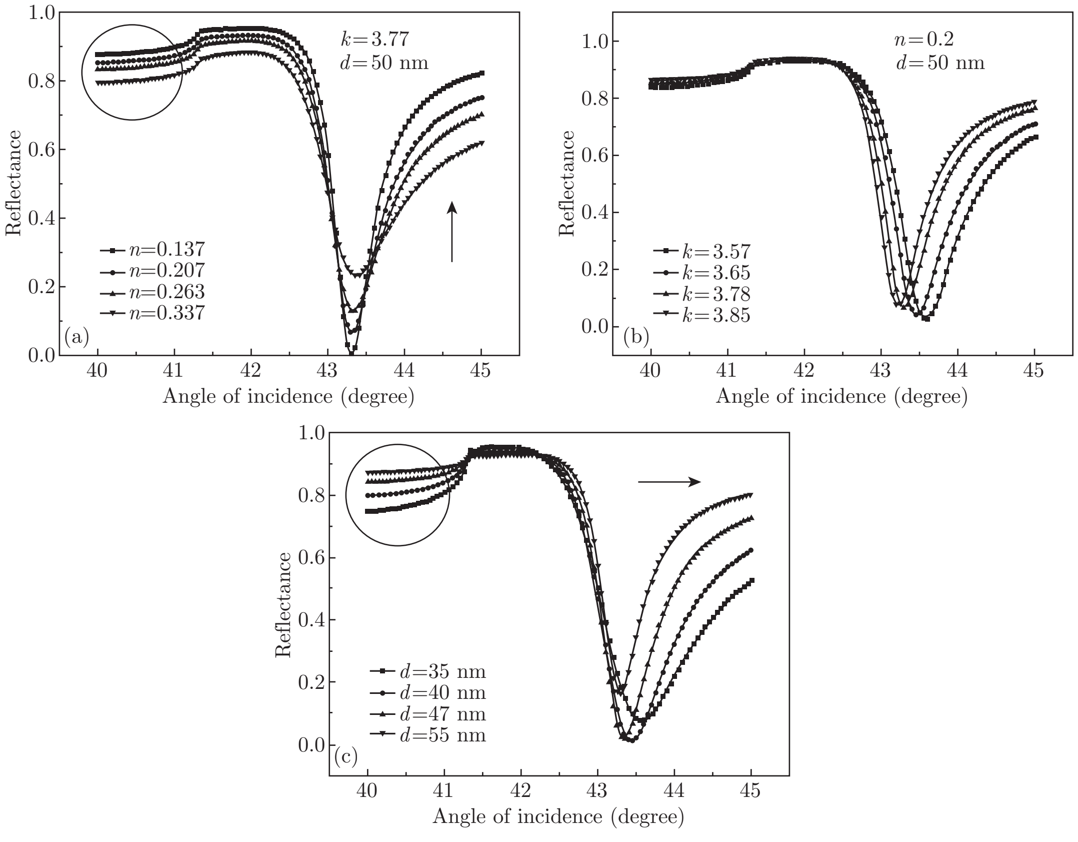

Fig. 2 SPR curves calculated taking into account a silver layer having different real part n of refractive index (a) and constant values of the imaginary part k and thickness d; different imaginary part k of refractive index (b) and constant values for n and d; different thickness d and constant values for n and k (c). The circled region shows the influence of n and d values to the shape of SPR curve in the region near the total internal reflection angle.

Figure 2 demonstrates also a dependence of the resonance peak angular position on the the extinction coefficient k. As can be seen, when extinction coefficient increases, a shift in the resonance angle to smaller angles takes place. In addition, the relationship between resonance curve and n, k and d values can be inferred from the observation of the curve in the ragion near the total internal reflection angle. It is quite clear that the d values variation results in a larger effect on the resonance curve than the n variation. The reflectivity measured at smaller angle value than the critical angle present a more significant relevance.

As can be seen from Fig. 3, the SPR curve for Ag-air interface shows a sharp dip in reflectance (symbol) at a resonance angle of 43.35°. Dip in reflectance curve is due to the excitation of SPW at Ag-air interface. The reflectance of a BK7 glass/Ag film/air system (metal film of thickness d_1) at an incident angle θ is given by Fresnel's equation [14].

$$R_{013} = \left| \frac{r_{01} r_{13} \exp(2ik_{z1}d_1)}{1 + r_{01} r_{13} \exp(2ik_{z1}d_1)} \right|^2, \tag{2}$$

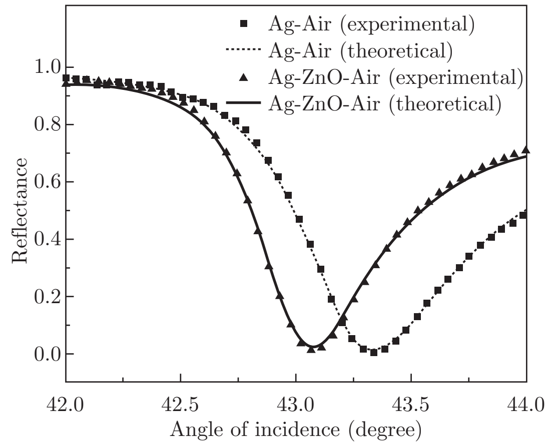

Fig. 3 SPR spectra for the BK7 glass/Ag film/air and BK7 glass/Ag film/ZnO/air system.

Where

$$r_{ik} = \left(\frac{k_{zi}}{\varepsilon_i} - \frac{k_{zk}}{\varepsilon_k} \right) \bigg/ \left(\frac{k_{zi}}{\varepsilon_i} + \frac{k_{zk}}{\varepsilon_k} \right), \tag{3}$$

and

$$k_{zi} = \frac{2\pi}{\lambda} \left(\varepsilon_i - \varepsilon_0 \sin^2 \theta \right), \tag{4}$$

where ε_0, ε_1, and ε_3 are dielectric constants of the prism materials, Ag film and air, respectively, and λ is the wavelength of incident light. For known values of ε_0 and ε_3 (1.515^2 and 1.0, respectively) the experimental SPR curve was fitted to simulation using Eq. (2), taking ε_1 (= $\varepsilon_1' + i\varepsilon_1$”) as the fitting parameters. ε_1' and ε_1” are varied until simulative SPR curve is fitted well to the experimental data. The best fitted simulative curve (dotted line) is shown in Fig. 3 for BK7 glass/Ag film/air system. The estimated value of ε_1 was about $-14.2 + i1.5$.

SPR curve relative to BK7 glass/Ag film/ZnO/air system is shown (symbol) in Fig. 3. Surface plasmon resonance angle obtained for the multilayer system having 200 nm as-deposited ZnO film was 43.06°. Dip in SPR reflectance curve is due to excitation of surface plasmons at Ag-ZnO interface. The internal incident angle θ_{spr} of the ZnO thin film exhibits a shift ($\sim 0.3°$) towards smaller angles than θ_{spr} for the bare Ag/BK7 glass. This change of the SPR curve is an indication of the change of plasmon resonance conditions due to the change in the refractive index when the Ag surface is covered by the ZnO thin film. The reflectance of the BK7 glass/Ag film/ZnO/air system corresponding to incident angle θ is given by [14].

$$R_{0123} = \left| \frac{r_{01} + r_{123} \exp(2ik_{z1}d_1)}{1 + r_{01} r_{123} \exp(2ik_{z1}d_1)} \right|^2, \tag{5}$$

where

$$r_{123} = \frac{r_{12} + r_{23} \exp(2ik_{z2}d_2)}{1 + r_{12} r_{23} \exp(2ik_{z2}d_2)}, \tag{6}$$

Where ε_2 and d_2 are complex dielectric constant and thickness of ZnO film, r_{ik} and k_{zi} are given by Eqs. (3) and (4), respectively. The subscripts 0, 1, 2 and 3 represent prism, Ag film, ZnO film and air respectively. The optical parameters of the Ag layer previously calculated have been used for the simulation procedure, to obtain information about the modifications induced in the SPR spectrum due to the presence of the ZnO film onto the Ag layer. ε_2(= $\varepsilon_2' + i\varepsilon_2$”) is obtained by fitting experimental SPR curve with simulation using Eq. (5). The real part of dielectric constant ε_2' is mainly determined by the θ_{spr} whereas the linewidth of resonance by the imaginary part of dielectric constant ε_2”. ε_2' and ε_2” are varied until the simulative curve (solid line), of the multilayer system, is fitted well to the experimental curve and the best fitting is shown in Fig. 3. The value of the complex dielectric constant (at $\lambda = 632.8$ nm) of the as deposited ZnO film extracted by the fitting procedure was $3.523 + i0.001$. Complex refractive index $(n_i + ik_i)$ was evaluated using the following relation:

$$n_i = \left[\frac{(\varepsilon_i^{'2} + \varepsilon_i^{''2})^{1/2} + \varepsilon_i^{'}}{2} \right]^{1/2}$$

$$k_i = \left[\frac{(\varepsilon_i^{'2} + \varepsilon_i^{''2})^{1/2} - \varepsilon_i^{'}}{2} \right]^{1/2}. \tag{7}$$

As can be seen in Fig. 4, a series of SPR reflectivity curves of the multilayer system related to samples of as-deposited and annealed at 100℃, 200℃, 300℃ and 400℃ were recorded. θ_{spr} of the BK7 glass/Ag film/ZnO/air system exhibits a shift from 43.06° to 44.27° with increase in temperature from 27℃ to 400℃, as shown in Fig. 5. Complex dielectric constant of ZnO film was estimated by fitting the experiment data with theory. As shown in Fig. 6, the values of ε_2' and ε_2'' are plotted as a function of temperature.

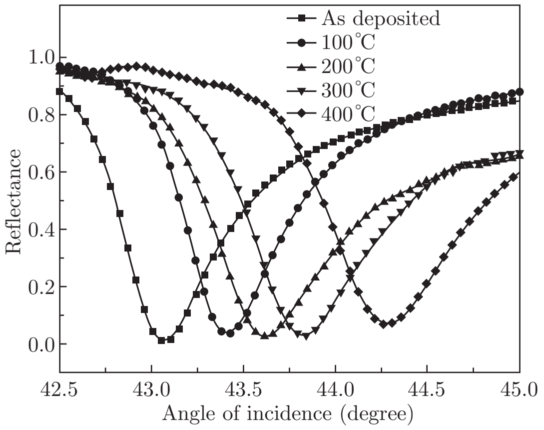

Fig. 4 SPR curves for BK7 glass/Ag film/ZnO/air system at different annealing temperature.

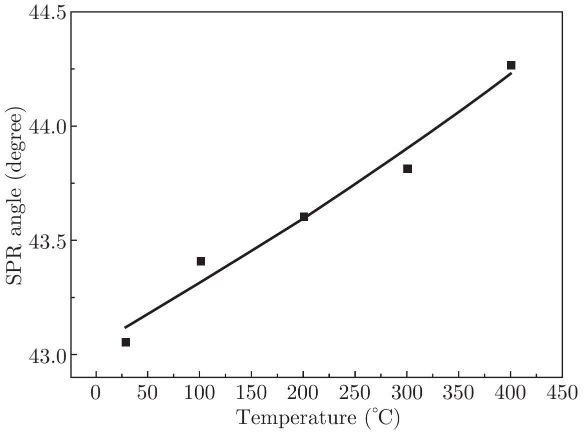

Fig. 5 Resonance angle (θ_{spr}) of the BK7 glass/Ag film/ ZnO/air system as a function of annealing temperature.

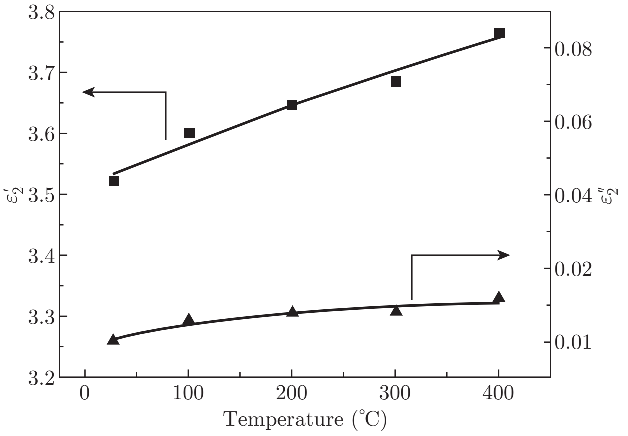

Fig. 6 Temperature variation of real and imaginary parts of dielectric constant of the ZnO film.

The magnitude of the shift in the θ_{spr} typically depends on both the thickness and the refractive index of the deposited ZnO layer. However, the effects of annealing temperature on the ZnO film thickness is not significant. Reports point that film thickness changes irreversibly with anneaning [17].

For easiness in seeing the Fig. 6, real part of dielectric constant of the ZnO film increase from 3.523 to 3.767 with increasing temperature from 27℃ to 400℃, whereas imaginary part of dielectric constant presented a slight increase with temperature. As can be seen in Fig. 7, an linear increase in n of ZnO film from 1.877 to 1.941 with increase in temperature from 27℃ to 400℃, whereas extinction coefficient shows a very small increase. Though the change in refractive index is 0.064 over a temperature range of 27℃ to 400℃, but the linearity and high accuracy of the SPR system shows its promising application as temperature sensor with a sensitivity of 1.8×10^{-4} RIU/℃. Generally, dense ZnO films with optical and structural homogeneity are desirable, since stability and reproducibility to the packing density. Film packing density can be seen in Fig. 7, which shows the dependence of the packing density on the annealing temperature calculated by using the following expression:

$$p = \frac{5}{3}\frac{n_f^2 - 1}{n_f^2 + 1}$$

where p is the film packing density, n_f the refractive index of ZnO films. Packing density increases with increase in annealing temperature. Thin films with low density have more grain boundaries and microvoids [18]. During the deposition, many of the atoms can be deposited at inappropriate positions. During the the annealing treatment, the atoms receive energy and migrate to relative equilibrium positions, which reduces the lattice strain, increases a more perfect crystallite and decreases the microvoids [19].

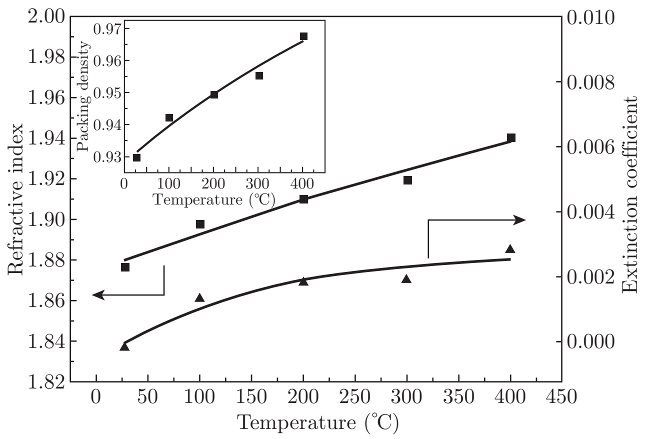

Fig. 7 Temperature variation of refractive index and extinction coefficient of ZnO thin film (inset: plot of packing density of ZnO film with annealing temperature).

Conclusions

Preparation and characterization of ZnO thin films onto suitable substrates for SPR measurement were performed. The annealing temperature dependence of dielectric propertites of ZnO films ($\lambda = 632.8$ nm) has been studied in the range 27–400℃ using the SPR technique in the Kretschmann configuration. The dielectric constant of ZnO films increases from $3.523+i0.001$ to $3.767+i0.011$ with increase in annealing temperature from 27 to 400℃. The corresponding increase in refractive index (1.877–1.941) and packing density (0.930–0.967) with increasing annealing temperature is attributed to the migration of atoms. The current results clearly indicate that SPR technique offer a real opportunity for studying the annealing temperature dependent optical properties of a dielectric thin film, and also could be used as a reliable temperature sensor.

Acknowledgments

This work was supported by Nano Special Plan from Shanghai Municipal Science and Technology Plan of Commission (grant no. 1052nm06900), and PhD Program Scholarship Fund of ECNU 2009. Ming Bao also wish to acknowledges the finacial support from the China Scholarship Council.

References

[1] C. Kittel, 7th. ed., Wiley, New York (1996).
[2] S. Kawata, Ed., Topics in Appl. Phys. 81, Springer-Verlag, Berlin (2001).
[3] V. M. Agranovich and D. L. Mills, eds., (North-Holland, 1982).
[4] B. Liedberg, C. Nylander and I. Lundstrum, Sens. Actuators B 4, 299 (1983).
[5] L. M. Zhang and D. Uttamchandani, Electron. Lett. 23, 1469 (1988).
[6] J. Homola, S. S. Yee and G. Gauglitz, Sens. Actuators B 54, 3 (1999).
[7] Ü. Özgür, Ya. I. Alivov, C. Liu, A. Teke, M. A. Reshchikov, S. Doğan, V. Avrutin, S. J. Cho and H. Morkoç, J. Appl. Phys. 98, 041301 (2005).
[8] R. Triboulet nad J. Perriere, Prog. Cryst. Growth Charact. Mater. 47, 65 (2003).
[9] A. Wei, X. W. Sun, J. X. Wang, Y. Lei, P. Cai, C. M. Li, Z. L. Dong and W. Huang, Appl. Phys. Lett. 89, 123902 (2006)
[10] C. Hanley, J. Layne, A. Punnoose, K. M. Reddy, I. Coombs, A. Coombs, K. Feris and D. Wingett, Nanotechnology 19, 295103 (2008).
[11] D. M. Bagnall, Y. F. Chen, Z. Zhu, T. Yao, S. Koyama, M. Y. Shen and T. Goto, Appl. Phys. Lett. 70, 2230 (1997).
[12] C. K. Ghosh, K. K. Chattopadhyay and M. K. Mitra, J. App. Phys. 101, 124911 (2007).
[13] M. Suchea, S. Christoulakis, K. Moschovis, N. Katsarakis and G. Kiriakidis, Thin Solid Films 515, 551 (2006).
[14] W. Water and S. and Y. Chu, Mater. Lett. 55, 67 (2002).
[15] E. Kretschmann, Z. Phys. 241, 313 (1971).
[16] F. S. Damos, R. C. S. Luz and L.T. Kubota, Langmuir 21, 602 (2005).
[17] A. G. Frutos, R. M. Corn, Anal. Chem. 70, 449A (1998).
[18] S. Ekgasit, C. Thammacharoen and W. Knoll, Anal. Chem. 76, 561 (2004).
[19] V. Gupta and A. Mansingh, J. Appl. Phys. 80, 1063 (1996).
[20] X. Hao, J. Ma, D. Zhang, T. Yang and J. Huang, Appl. Surf. Sci. 183, 137 (2001).
[21] Y. M. Lu, W. S. Hwang, W. Y. Liu and J. S. Yang, Mater. Chem. Phys. 72, 269 (2001).